Ecological Applications, 27(8), 2017, pp. 2514–2527

Climatic and anthropogenic drivers of northern Amazon fires during the 2015–2016 El Niño event

Marisa G. Fonseca,[1,7] Liana O. Anderson,[2,3] Egidio Arai,[1] Yosio E. Shimabukuro,[1] Haron A. M. Xaud,[4] Maristela R. Xaud,[4] Nima Madani,[5] Fabien H. Wagner,[1] and Luiz E. O. C. Aragão[1,6]

[1]*Tropical Ecosystems and Environmental Sciences Laboratory (TREES), National Institute for Space Research (INPE), Av. dos Astronautas, 1758, 12227-010 São José dos Campos, SP Brazil*
[2]*National Center for Monitoring and Early Warning of Natural Disasters (CEMADEN), Parque Tecnológico de São José dos Campos, Estrada Dr. Altino Bondensan 500, 12247-016 São José dos Campos, SP Brazil*
[3]*Environmental Change Institute, ECI, University of Oxford, South Parks Road, Oxford OX1 3QY United Kingdom*
[4]*Brazilian Agricultural Research Corporation, Embrapa Roraima, PO Box 133, 69.301-970 Boa Vista, RR Brazil*
[5]*Numerical Terradynamic Simulation Group, College of Forestry & Conservation, University of Montana, Missoula, Montana 59812 USA*
[6]*College of Life and Environmental Sciences, University of Exeter, Exeter EX4 4RJ United Kingdom*

Abstract. The strong El Niño Southern Oscillation (ENSO) event that occurred in 2015–2016 caused extreme drought in the northern Brazilian Amazon, especially in the state of Roraima, increasing fire occurrence. Here we map the extent of precipitation and fire anomalies and quantify the effects of climatic and anthropogenic drivers on fire occurrence during the 2015–2016 dry season (from December 2015 to March 2016) in the state of Roraima. To achieve these objectives we first estimated the spatial pattern of precipitation anomalies, based on long-term data from the TRMM (Tropical Rainfall Measuring Mission), and the fire anomaly, based on MODIS (Moderate Resolution Imaging Spectroradiometer) active fire detections during the referred period. Then, we integrated climatic and anthropogenic drivers in a Maximum Entropy (MaxEnt) model to quantify fire probability, assessing (1) the model accuracy during the 2015–2016 and the 2016–2017 dry seasons; (2) the relative importance of each predictor variable on the model predictive performance; and (3) the response curves, showing how each environmental variable affects the fire probability. Approximately 59% (132,900 km^2) of the study area was exposed to precipitation anomalies ≤ -1 standard deviation (SD) in January and ~48% (~106,800 km^2) in March. About 38% (86,200 km^2) of the study area experienced fire anomalies ≥ 1 SD in at least one month between December 2015 and March 2016. The distance to roads and the direct ENSO effect on fire occurrence were the two most influential variables on model predictive performance. Despite the improvement of governmental actions of fire prevention and firefighting in Roraima since the last intense ENSO event (1997–1998), we show that fire still gets out of control in the state during extreme drought events. Our results indicate that if no prevention actions are undertaken, future road network expansion and a climate-induced increase in water stress will amplify fire occurrence in the northern Amazon, even in its humid dense forests. As an additional outcome of our analysis, we conclude that the model and the data we used may help to guide on-the-ground fire-prevention actions and firefighting planning and therefore minimize fire-related ecosystems degradation, economic losses and carbon emissions in Roraima.

Key words: anthropogenic ignition; climate; fire modeling; hot pixels; machine learning; multivariate ENSO index; savannas; tropical forests.

Introduction

Fire has long been used for land management and other subsistence activities by indigenous populations, influencing soil characteristics, vegetation composition, and the dynamics of Amazonian forests since pre-Columbian times (Bush et al. 2008, Schwartzman et al. 2013). In the state of Roraima, located in the northernmost part of the Brazilian Amazon (Fig. 1), integrated pollen and sedimentological records suggest that, despite the moist conditions in the last 1,050 yr (Meneses et al. 2013), human-ignited fire has markedly influenced the boundaries between forest and savanna areas, killing pioneer forest species invading savanna areas and hence hampering forest expansion (Meneses et al. 2015). Conversely, an expansion of forests was reported in certain areas of the state after 200 cal yr BP, allegedly because of the decline and displacement of indigenous populations after the arrival of European settlers and consequent reduction in fire occurrence (Meneses et al. 2013, 2015). On the other hand, the analysis of charcoal concentrations of surface sediments in the forest–savanna transition of this region

Manuscript received 15 December 2016; revised 18 July 2017; accepted 28 July 2017. Corresponding Editor: David S. Schimel.
[7] E-mail: marisa_fonseca@yahoo.com.br

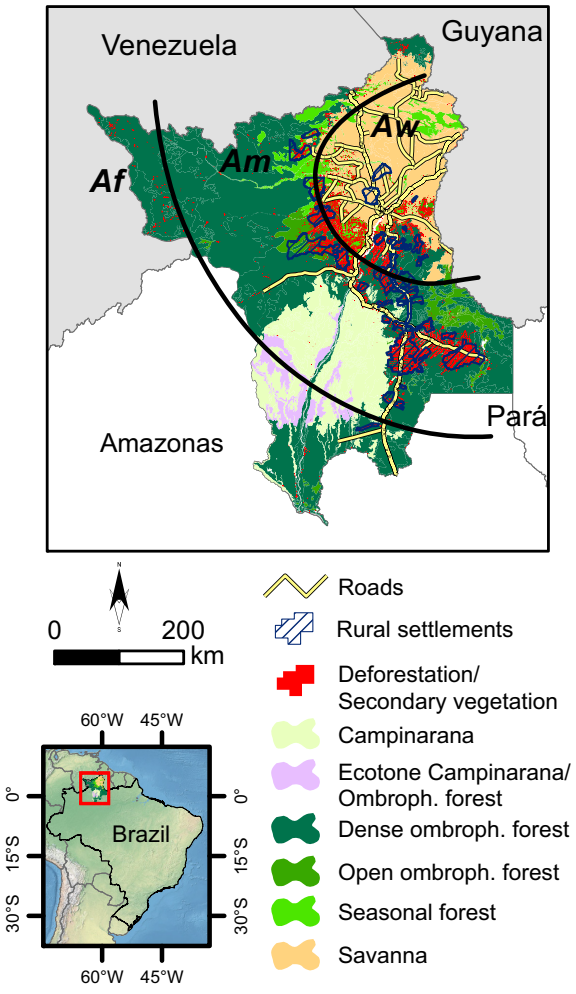

FIG. 1. Roraima state map showing the road network, rural settlements, native vegetation cover, and deforestation/secondary vegetation (total area deforested until 2014 with or without secondary vegetation growing over it; see the *Study area* and *Data sets* sections for cartographic data sources). Curved black lines indicate the Köppen climate classification: Af, equatorial climate; Am, monsoonal climate and Aw tropical savanna climate. Ombroph., Ombrophilous. [Color figure can be viewed at wileyonlinelibrary.com]

indicated that forest cover acted as an effective buffer during the last millennium, blocking fire entrance into forested ecosystems (Meneses et al. 2015). As in other parts of Amazonia, forest fires were probably a rare event in Roraima before the 20th century (Schroeder et al. 2013).

The synergy between intense drought events and modern human activities may be causing new changes in the landscape dynamics and in the carbon emissions from this region (Barbosa and Fearnside 1999, Bush et al. 2008, Barni et al. 2015*b*). In the 1997–1998 El Niño event, approximately 11,000 to 14,000 km^2 of forests were burned in the state of Roraima, an area equivalent to 7.4–9.0% of its forest cover and over twice as large as the total deforested area in the state up to 1997 (Barbosa and Fearnside 1999). Elvidge et al. (2001) estimated a 20-fold increase in the area of heavily burned forest in 1997–1998 (9,038 km^2) compared to 1995, a typical year in terms of precipitation, when only 425 km^2 of forests were burned. In 2003, a moderate El Niño event was also associated with an increase of forest fires in the state. A rough estimate from Barbosa et al. (2004) suggested that 85 km^2 of primary forests were affected per day by fire between February and March 2003 in Roraima.

During the strong 2015–2016 El Niño Southern Oscillation (ENSO) event, record-breaking warming and extreme drought were observed in the northern Brazilian Amazon, especially in the state of Roraima (Jiménez-Muñoz et al. 2016). The Multivariate ENSO Index (MEI) values during December 2015–January 2016 and January–February 2016 were among the three highest values since 1950, being only slightly lower than 1997–1998 and 1982–1983 values (data *available online*).[8] The occurrence of fire in the state of Roraima reached a peak in January 2016, when the number of active fires detected by satellite sensors was over six times the mean number for that month and the highest for any month since September 1998, when this data became available (INPE 2016). However, an in-depth analysis of the magnitude and spatial pattern of precipitation and fire anomalies in Roraima during the 2015–2016 event has not been performed yet.

The positive feedbacks between intense drought events, land use, and fire have been widely addressed in the literature (e.g., Nepstad et al. 2001, Davidson et al. 2012, Anderson et al. 2015). In the state of Roraima, the construction of two major roads (BR-174 and BR-210) at the end of the 1970s fostered the region's occupation, enabling the establishment of rural settlements in previously isolated areas (Diniz and Santos 2005). Additionally, governmental programs provided incentives for population immigration, in an attempt to both occupy the region and to reduce conflicts related to land tenure in the Brazilian Northeast and Southeast regions (Barbosa 1993). Due to fire being the main practice used in the Brazilian Amazon to clear land during the deforestation process, to remove secondary vegetation and to renew pastures, the expansion of occupation frontiers widely increased ignition sources across the state. Furthermore, secondary vegetation growing in previously deforested areas is highly prone to accidental fires given its short and opened canopy (Ray et al. 2005), mostly in its early regeneration stages and in dry years (Gutiérrez-Vélez et al. 2014). Barni et al. (2015*b*) estimated that 3.06×10^3 km^2 has been deforested and 3.02×10^3 km^2 of forests have burned between 2000 and 2010 in Roraima. These authors found that 98.5% of the forest area affected by fire was burned in years with El Niño events. The detrimental effects of fires on forest structure, biomass, and floristic composition in Roraima were documented by Martins et al. (2012) and Xaud et al. (2013).

[8] http://www.esrl.noaa.gov/psd/enso/mei/table.html

The current availability of remote sensing data offers the opportunity to integrate updated information from multiple sources to model fire occurrence over extensive and remote areas of the Amazon. For the Brazilian Amazon, spatially explicit annual deforestation and supra-annual land-use data derived from remote sensing are produced and publicly shared by governmental programs. These data can be used together with maps of other anthropogenic variables (such as roads and rural settlements) and satellite-based precipitation data to investigate the influence of such drivers on fire occurrence.

Satellite-derived data is also a valuable source of near-real-time information on active fires, especially in the remote and vast areas of the Amazon ecosystems. From a fire modeling perspective, although satellite-based active fire detections indicate the locations that are being burned at the time of the detection, it is not possible to determine whether other areas were also suitable to burn at that time but did not due to the lack of an ignition source. Furthermore, omission errors may occur when using passive remote sensing due to thick cloud cover, frequent in this region (Schroeder et al. 2008), when the fire started and ended between the satellite passages or when it was not hot enough to be detected by the thermal sensors onboard the satellite. Therefore, as the absence of fire suitability cannot be accurately mapped using satellite-based fire detections, it is appropriate to use an approach that rely only on presence data to model fire suitability (Peters et al. 2013).

The Maximum Entropy method (MaxEnt) was introduced in ecological studies based on presence-only data by Phillips et al. (2004, 2006) and was successfully applied to model fire occurrence in the Brazilian Amazon (Fonseca et al. 2016) and elsewhere (Parisien and Moritz 2009, Moritz et al. 2012, Parisien et al. 2012, Renard et al. 2012, Bar Massada et al. 2013, Paritsis et al. 2013, Peters et al. 2013, Arnold et al. 2014). This model allows for an integration of climatic and anthropogenic variables and may be useful for understanding the relative importance of these variables and for supporting planning and decision making in firefighting and fire prevention (Fonseca et al. 2016).

Although MaxEnt's accuracy and the relative contribution of variables for fire prediction was already estimated for the Brazilian Amazon by Fonseca et al. (2016), a gap in the knowledge concerning fire modeling in the state of Roraima still remains given that: (1) the previous model was tested for the period between June and November, when the dry season in most of the Brazilian Amazon occurs. However, as most of Roraima's territory is located in the Northern Hemisphere, the peak of fire in the state occurs between December and March, and was not covered, therefore, by the previous study; (2) the previous model was calibrated for 2010, when the drought was associated with the warming of the tropical Atlantic Ocean, with effects mostly in the western and southern regions of the Amazon (Fernandes et al. 2011, Lewis et al. 2011) but not in the Northern Amazon, where Roraima is located; (3) the previous model did not include non-forest vegetation areas, which represent a significant proportion of the Roraima state; and (4) the relative importance of predictor variables may vary among spatial scales (e.g., Parisien and Moritz 2009, Renard et al. 2012). Understanding this variation may provide important insights into fire occurrence.

Here we map the extent of precipitation and fire anomalies during the extreme 2015–2016 ENSO and quantify the effects of climatic and anthropogenic drivers on fire occurrence in the state of Roraima. We also test the accuracy of the fire-probability model during the 2015–2016 and 2016–2017 fire seasons (from December to March) aiming to support future planning and decision-making in firefighting and fire prevention in Roraima. In order to achieve these objectives, we first estimate and compare the spatial pattern of the anomaly of precipitation based on data from the Tropical Rainfall Measuring Mission (TRMM), and the anomaly of fire occurrence, based on the active fires detection (hereafter hot pixels) data of the Moderate Resolution Imaging Spectroradiometer (MODIS) sensor aboard the AQUA satellite in the 2015–2016 fire season. Then, we integrate climatic and anthropogenic drivers in a model of fire probability in Roraima using the MaxEnt to quantify (1) the model accuracy, (2) the relative importance of each predictor variable on the overall model predictive performance, and (3) the response curves, showing how each environmental variable affects the model prediction. The present model was built in a finer spatial scale (0.1°) compared to the Fonseca et al. (2016) study (0.25°), which improves its ability to support planning and decision-making in firefighting and fire prevention in Roraima.

Methods

Study area

The state of Roraima is located in the northern Brazilian Amazon, sharing borders with Venezuela in the northwest, Guyana in the northeast, and the Brazilian states of Pará and Amazonas in the south (Fig. 1). Roraima's territory extends over ~ 224,300 km^2, an area approximately the size of the United Kingdom (~242,000 km^2). Annual precipitation increases from the northeast (1,100–1,400 mm/yr), where a large mosaic of savanna ecosystems occur, to the lowland dense forests in the southernmost part of the state (2,000–2,300 mm/yr; Barbosa 1997). In the south, there is small month-to-month precipitation variation and the climate is classified as equatorial (Af) following the Köppen system. The northeast, under a tropical savanna climate (Aw), experiences a well-defined dry season, with approximately 10% of the annual rainfall and high incidence of solar radiation (between 160 and 200 h of insolation/month) between December and March (Barbosa 1997). In the transition zone, with a monsoonal climate (Am), a dry season occurs in the same months, although

less extreme than in the region under the Aw climate. Besides the dense ombrophilous forests (i.e., forest occurring under high precipitation and between 0 and 60 d without rainfall), there are patches of open ombrophilous and seasonal forests, and in the central-southern portion of the state, sandy soils give rise to the *Campinarana* vegetation, which encompass a distinct mosaic of vegetation physiognomies ranging from grasslands to forests (IBGE 2012). Fire occurrence shows a marked seasonality in the state. From 1999 to 2015, the period between December and March experienced between 52% and 91% of the total annual hot pixels, except for 2009, when ~40% of the annual hot pixels were detected during this period (data *available online*).[9]

Data sets

To estimate the anomaly of fire occurrence in the 2015–2016 fire season we used the afternoon detections of hot pixel data detected from the MODIS sensor onboard the AQUA satellite, published online by the Fire Monitoring Project from the Centre for Weather Forecast and Climate Studies (CPTEC) of Brazil's National Institute for Space Research (INPE) (see footnote 9). Hot pixels consist of the signal detection of the radiance of fire flames, whose emission peak is situated in the middle infrared region. MODIS spatial resolution is 1 km, daily temporal resolution. A flaming fire front of at least 30 m × 1 m of extension or larger are detected by MODIS sensor[10]. Smaller or short-lived fires (occurring between satellite passages) or the ones occurring under dense vegetation cover, on cloudy days, or on the mountain face opposite to the satellite position may not be detected. No information on the burned area is provided with the hot pixels' data.

As the number of satellites and the quality of some of their data vary along time, for temporal analysis such as fire anomalies, it is important to use hot pixels from only one satellite that present consistent data collection during the analyzed period. However, for the fire modeling calibration, which requires only one month of data, we used hot pixels detected by all satellites available at the INPE Fire Monitoring Project's website (see footnote 9) in order to avoid underestimation of fire occurrence, namely the National Oceanic and Atmospheric Administration (NOAA) family of satellites, the satellites 8, 10, 12, and 13 of the Geostationary Operational Environmental Satellite Program (GOES), AQUA, TERRA, Meteosat-2, Suomi National Polar-orbiting Partnership satellite (NPP), and the Along Track Scanning Radiometer (ATSR).

MEI values, which combine six observed variables over the tropical Pacific (sea-level pressure, zonal and meridional components of the surface wind, sea surface temperature, surface air temperature, and total cloudiness fraction of the sky) were obtained and used to estimate the effect of ENSO on fire occurrence (data *available online*).

In order to estimate long-term precipitation anomalies, we used the TRMM 3B43 7A product, which has 0.25° of spatial resolution, from January 1998 until March 2016 (available *online*).[11] Although the precipitation radar of the TRMM satellite stopped collecting data on October 2014, the continuity of the 3B43 product was accomplished by an adaptation of the climatological calibrations/adjustments scheme of the real-time version of TMPA (TRMM Multi satellite precipitation analysis), with minimal impact on the estimates over land due to the continued inclusion of gauge analysis (Bolvin and Huffman 2015).

Since 2015, the Global Precipitation Measurement (GPM) Mission has been publicly providing near-real-time estimates of precipitation through the Integrated Multi-satellite Retrievals for GPM (IMERG) data product[12]. Therefore, for the fire modeling, we used the late-run near-real-time IMERG product, since this data is produced with approximately 16 h of latency and therefore is most suitable for future short-term fire modeling purposes than either the post-real-time research IMERG (which is made available approximately three months after the observation month) or 3B43 products. IMERG precipitation data with a spatial resolution of 0.1° were obtained from NASA (data *available online*).[13] As images of precipitation accumulation up to 7 d are available in this data version, we added the accumulated images in each month in order to estimate monthly precipitation. Estimates of IMERG accuracy are still scarce and concerns mostly the post-real-time research product (Huffman et al. 2015, Chen and Li 2016, Liu 2016, Prakash et al. 2016, Sharifi et al. 2016). We therefore carried out a preliminary assessment of the late-run near-real-time IMERG product accuracy over the state of Roraima using monthly rain gauge data from April 2015 until March 2016 from the only two weather stations with updated data at the time of the analysis publicly available for Roraima state, named Boa Vista (02°49′12″ N 60°39′36″ W) and Caracaraí (01°49′48″ N 61°07′12″ W) (obtained from the Brazilian National Institute of Meteorology; available *online*).[14] The coefficients of determination (r^2) of the linear regressions between monthly near-real-time late-run IMERG and rain gauge data were 0.799 and 0.959 for the Boa Vista and Caracaraí stations, respectively, which suggests that the IMERG data is suitable for our purposes.

The land-use related variables included in the fire modeling were (1) recent deforestation, recorded between August 2013 and July 2014 by the INPE's

[9] http://www.inpe.br/queimadas

[10] http://www.inpe.br/queimadas/faq.php

[11] http://mirador.gsfc.nasa.gov

[12] http://pmm.nasa.gov/resources/documents/gpm-integrated-multi-satellite-retrievals-gpm-imerg-algorithm-theoretical-basis-

[13] https://pmm.nasa.gov/data-access/downloads/gpm

[14] http://www.inmet.gov.br/projetos/rede/pesquisa/

PRODES project (Amazon Deforestation Monitoring Project, this data refers to clearing of old-growth forest vegetation only; available *online*);[15] (2) secondary vegetation map (vegetation growing in previously deforested areas mapped by PRODES) produced by INPE's TERRACLASS Program (Mapping land use and land cover in the Brazilian Amazon Program, available *online*);[16] (3) distance to the roads network (road network vector file *available online*);[17] and (4) rural settlements (INCRA 2015; file *available online*).[18] Additionally, we used the map of the area originally covered by non-forest vegetation, i.e., open vegetation types represented by savannas, floodplain vegetation, and most of the *Campinarana* cover, in the state from the TERRACLASS Program. Unfortunately no data on the clearing of such vegetation types is available.

Precipitation and fire anomalies

The pixel-by-pixel mean and standard deviation of monthly precipitation were calculated for Roraima using TRMM 3B43 data from 1998 until 2014, but excluding the precipitation in 2005 and 2010, two years of intense drought events in the Brazilian Amazon (Lewis et al. 2011, Marengo et al. 2011). The 2005 drought event was considered one of the most severe in the previous 100 yr (Marengo et al. 2008) and in 2010 another drought even more spatially extensive struck the region (Lewis et al. 2011, Marengo et al. 2011). Therefore, the exclusion of these two years from the 17-yr time series analyzed aims to avoid the underestimation of the historical average precipitation. The monthly precipitation anomalies from December 2015 to March 2016 were then calculated as the departure from the considered time-series mean, normalized by the standard deviation. Additionally, the precipitation anomalies from January to March 1998 were calculated for comparison with the last strong El Niño event.

The monthly number of MODIS hot pixels for each grid cell with 0.25° × 0.25° of spatial resolution was derived by aggregating the daily observations and the pixel-based fire anomalies were calculated using the same method to derive the rainfall anomaly, but using a time-series starting in 2003, when the first whole-year data was available.

Modeling fire drivers

For the fire modeling using MaxEnt, the study area was divided into a 0.1° resolution grid, since this is the spatial resolution of the near-real-time precipitation data we used (see *Data sets*). As climatic variables, besides the monthly precipitation obtained from IMERG data, we produced monthly spatially explicit information on the sensitivity of grid cells to changes in MEI in terms of fire occurrence. For that purpose, the monthly pixel-based fire anomalies were calculated in 0.1° grid cells from 2003 to 2015 using the same procedure described above. For each individual 0.1° grid cell, we then calculated the slope and intercept coefficients of a linear model of fire anomaly as a function of MEI during the referred period. To be able to represent over the space the impact of SST changes on fire patterns for each month analyzed, for each of these grid cells we then applied the pixel-based linear model

$$\mathrm{EEI}_{(i,j)} = a_{(i,j)} + b_{(i,j)}(\mathrm{MEI}) \quad (1)$$

where $\mathrm{EEI}_{(i,j)}$ is the ENSO effect index, i.e., a monthly proxy of the Pacific SST anomaly effect on fire occurrence within each grid cell with i latitude and j longitude, MEI is the bimonthly value of the Multivariate ENSO Index, a is the intercept, and b is the slope obtained from the fit of the linear regression. The parameters a and b are spatially variable but temporally static.

We tested the effect of including vapor pressure deficit (VPD) data as a predictor variable, given that it has previously been shown to influence Amazonian fire conditions (e.g., Silvestrini et al. 2011). We calculated the average monthly VPD from the daily air temperature and dew point data (Murray 1967) obtained from the Modern-Era Retrospective Analysis for Research and Applications Version 2 (MERRA-2; Zomer et al. 2008). However, the projected surfaces of suitability for fire occurrence, which varies from zero to one, were similar using the models with and without VPD (92.8%, 96.9%, 94.8%, and 92.9% of the grid cells differed from −0.05 to 0.05 between the two models for December 2015, January, February, and March 2016, respectively). As we aim to use the model operationally, the final model does not include the VPD since including it would increase the data processing time, without contributing significantly to the detection of areas of high fire incidence probability.

For all land-use land-cover variables except distance to roads (recent deforestation, secondary vegetation, settlement areas, and original non-forest vegetation), the aggregation process into 0.1° grid cells consisted in calculating the fractional area covered by each category in each grid cell. Pasture was initially considered as a variable to be included in the model, but it showed high correlation with secondary vegetation ($r_{\mathrm{pearson}} = 0.83$) and, based on preliminary jackknife tests to estimate model performance using each variable individually, it was excluded. Pearson's correlation coefficient between all other variables mentioned above were below 0.6 and they were kept in the model (Parisien and Moritz 2009).

January 2016 was chosen for model calibration because it was the peak of 2015–2016 fire season in the state of Roraima, providing a wide range of environmental

[15] http://www.obt.inpe.br/prodes/index.php

[16] http://www.inpe.br/cra/projetos_pesquisas/dados_terraclass.php

[17] http://mapas.mma.gov.br/i3geo/datadownload.htm

[18] http://acervofundiario.incra.gov.br/i3geo/datadownload.htm

conditions driving fire occurrence. Therefore, for model calibration, we used hot pixels from January 2016, climatic data from December 2015, recent annual deforestation between 2013 and 2014, and secondary vegetation map from 2012. Each grid cell with three or more hot pixels in January 2016 was used only once in model calibration, avoiding pixel oversampling (Phillips and Dudik 2008, Couturier et al. 2014, Giovannini et al. 2014). The chosen threshold for a fire event to be included in model calibration (three or more hot pixels) correspond to the third quartile of the distribution of the number of hot pixels per grid cell in that month in Roraima, in an attempt to model the occurrence of the most significant fire events (longer lasting or over larger areas; Fonseca et al. 2016).

The analysis was carried out using the MaxEnt software version 3.3.3 (Phillips et al. 2004, 2006). The software logistic output was used, which can be interpreted as a normalized suitability surface with values ranging from zero to one, equivalent to a relative (rather than absolute) probability of fire occurrence. MaxEnt uses the values of the predictor variables at the occurrence records and a random sample of their values across the landscape (typically called a background sample) to estimate the target probability distribution of maximum entropy (i.e., that is most spread out or closest to uniform) subject to a set of constraints (Phillips et al. 2006). The predictor variables and mathematical transformations thereof are called "features," and the constraints are that the expected value of the features should be close to its empirical average at the sample points (here, hot pixel occurrence). The transformations can be linear, quadratic, product (equivalent to interaction terms in regression), threshold or hinge (similar to threshold, except that a linear function is used). A user-defined constant called regularization multiplier reduces overfitting by ensuring that the empirical constraints are not fit too precisely and removing features from the model. We first compared the model predictive performance using the metric test area under the curve (AUC) while setting the regularization multiplier from 1 to 4. As the difference found in the test AUC was in the third decimal place, we set this value to one, which is the default value of the software. We used bootstrap resampling technique with 50 runs to estimate the outputs mean and standard deviation (Verbyla and Litvaitis 1989), setting aside 30% of sample points for model testing. We then used the calibrated model to simulate the probability of fire occurrence and test its accuracy for the 2015–2016 (from December 2015 until March 2016) and 2016–2017 (from December 2016 until March 2017) fire seasons in the state by substituting EEI and precipitation data by data from one month prior to the simulated month. Considering that in the 2016–2107 fire season the temperature of the Pacific ocean had already cooled down and the active fire detection was lower than in the previous season (see *Results*), analyzing the model accuracy during both periods provides a test of its performance under different conditions.

In modeling using MaxEnt, a final map of fire predicted occurrence can be produced based on a threshold suitability value, above which fire is predicted to occur. The classifier sensitivity for a particular threshold is the fraction of all occurrence records that are correctly predicted as occurrence instances by the classifier and is also called the true positive rate, representing absence of omission error. Specificity is the fraction of all absence instances that are correctly predicted as such by the classifier and the quantity 1 − specificity, also known as the false positive rate, represents commission error (Fielding and Bell 1997, Phillips et al. 2006). As a threshold-independent measure of model performance, the Receiver Operating Characteristic (ROC) curve is obtained by plotting sensitivity on the y-axis and 1 − specificity on the x-axis for all possible thresholds and the AUC value quantifies the probability that the model correctly ranks a random presence locality higher than a random background site (Phillips et al. 2006). If the AUC value is 0.5, the model is no better than random, while an area with a value close to 1 indicates an accurate model (Fielding and Bell 1997). Models with AUC values above 0.75 are considered potentially useful (Elith 2002). We present the calibration and test AUC values averaged over the 50 replicate runs and its standard deviation and model sensitivity and false positive rates, calculated based on the actual hot pixel occurrence in the simulated month, for thresholds from 0.2 up to 0.7, in intervals of 0.1. As we have only pseudo-absence data, the false positive rate may be overestimated. In order to estimate which variables are most important for model predictive performance, we used the jackknife test and assessed test AUC values for models created using each variable individually (Elith et al. 2011). We also assessed how each variable affects the MaxEnt prediction using response curves (Elith et al. 2011). The curves show how the suitability (as measured by the software logistic output) changes as each environmental variable is varied, keeping all other environmental variables at their average sample value.

Results

Precipitation and fire anomalies

Based on TRMM estimates, mean precipitation values in the state of Roraima were 16.8, 3.2, 33.8, and 69.4 mm in December 2015, January, February, and March 2016, respectively. January and March 2016 were the months with the larger extent of (negative) precipitation and (positive) fire anomalies (Fig. 2). However, precipitation anomaly was more spatially extensive than fire anomaly, reaching ~132,900 km^2 (~59% of the state area) with anomaly ≤−1 SD in January and ~106,800 km^2 (~48% of the state area) in March. Approximately 81% of the state area experienced rain anomaly ≤−1 SD in at least one month between December 2015 and March 2016.

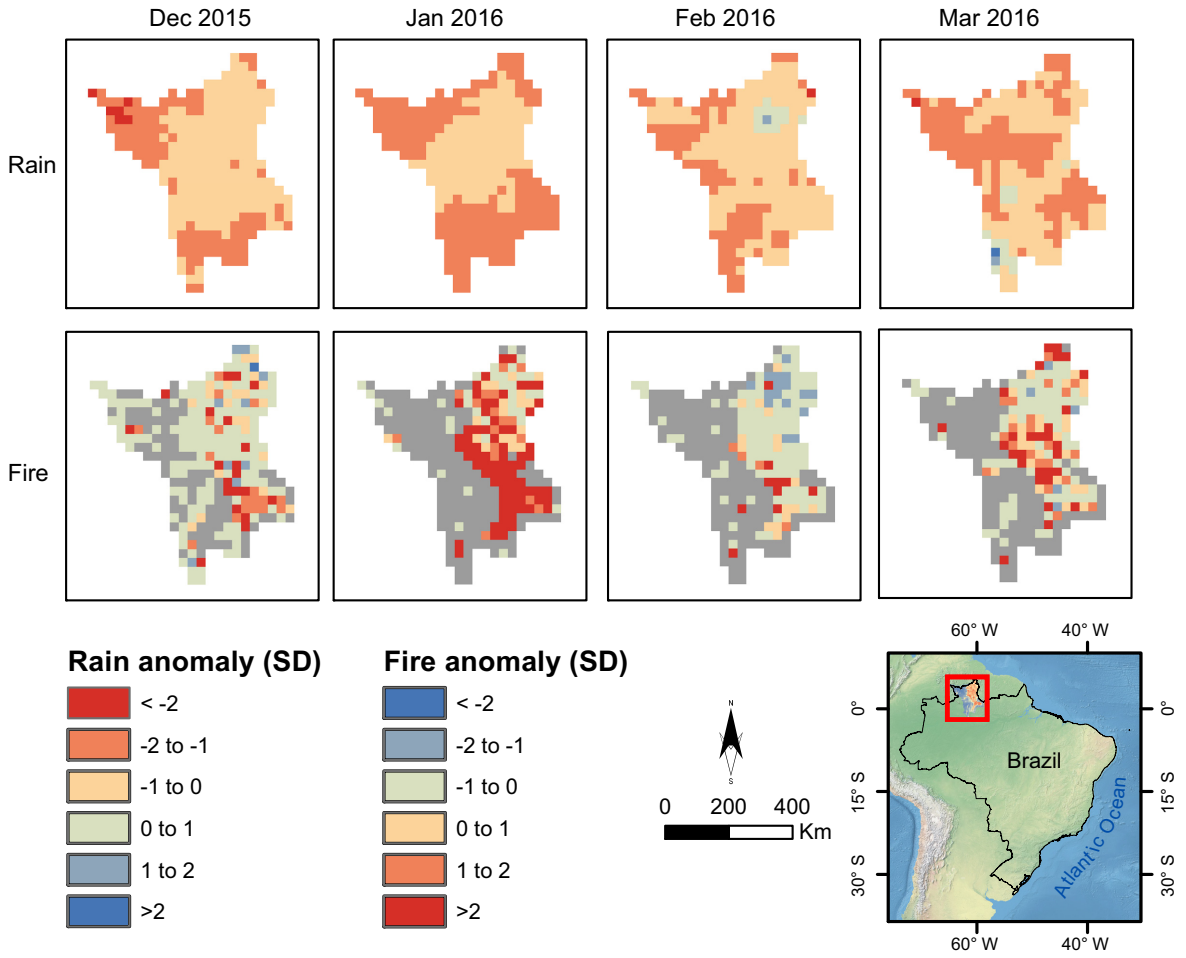

FIG. 2. Satellite-derived standardized anomalies for rainfall and fire detections from December 2015 until March 2016 in Roraima state. Gray areas did not show fire detection in that month during the analyzed period. [Color figure can be viewed at wileyonlinelibrary.com]

The 3B43 data is available since January 1998 and, using this data, we estimate that mean precipitation in the state of Roraima was higher in January and February 1998 (19.8 and 50.4 mm, respectively), and lower in March 1998 (48.2 mm) than in same months of 2016. Accordingly, the proportion of the state under precipitation anomaly ≤ -1 SD followed the same pattern (26, 11 and 70% in January, February, and March 1998 compared to 59%, 31%, and 48% in the same months of 2016).

AQUA MODIS fire detection reached 1,754 hot pixels in January and 1,081 in March 2016 in Roraima. Approximately 67,900 km^2 (~30% of the state area) showed positive fire anomaly ≥ 1 SD in January 2016, mostly concentrated in the oriental part of the state (Fig. 2). In March 2016, fire anomaly ≥ 1 SD was observed in ~37,400 km^2 (~17%) and it was mostly concentrated in the central area of the state. About 38% (86,200 km^2) of the state area experienced fire anomaly ≥ 1 SD in at least one month between December 2015 and March 2016.

Modeling fire drivers

The average training AUC for the replicate runs and its standard deviation was 0.837 $\pm$ 0.008 while average test AUC value was 0.807 $\pm$ 0.012, indicating satisfactory model performance. The monthly number of grid cells with three or more hot pixels varied between 202 and 525 during the 2015–2016 fire season and between 127 and 254 during the 2016–2017 fire season. The suitability surfaces predicted by the model and the maps of grid cells with three or more hot pixels in the two fire seasons are presented in Fig. 3. The distribution of suitability values was significantly higher in grid cells where three or more hot pixels were subsequently detected compared to grid cells with two or fewer hot pixels for both fire seasons (Fig. 4).

Lower threshold values have higher sensitivity (true positive rate) but also a higher false positive rate, as expected (Fig. 5). The sensitivities of model projections were higher than 0.78 for all months analyzed except February 2016

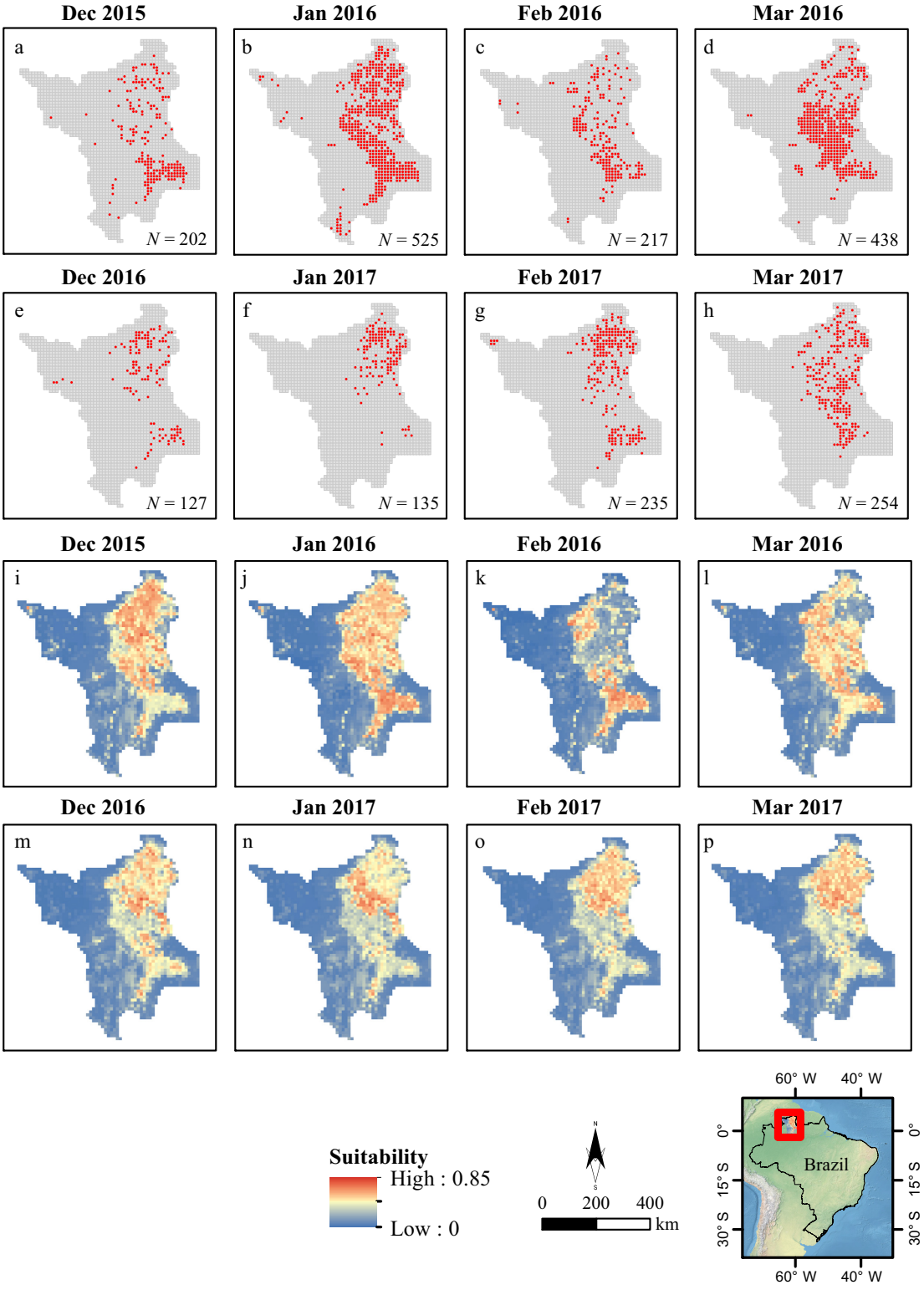

FIG. 3. Maps of grid cells with three or more hot pixels during the two studied fire seasons (a–d, from December 2015 until March 2016 and e–h, from December 2016 until March 2017; numbers in the lower right refer to grid cell counts) and surfaces of suitability for fire occurrence projected by the model for these months (i–p) in the state of Roraima. [Color figure can be viewed at wileyonlinelibrary.com]

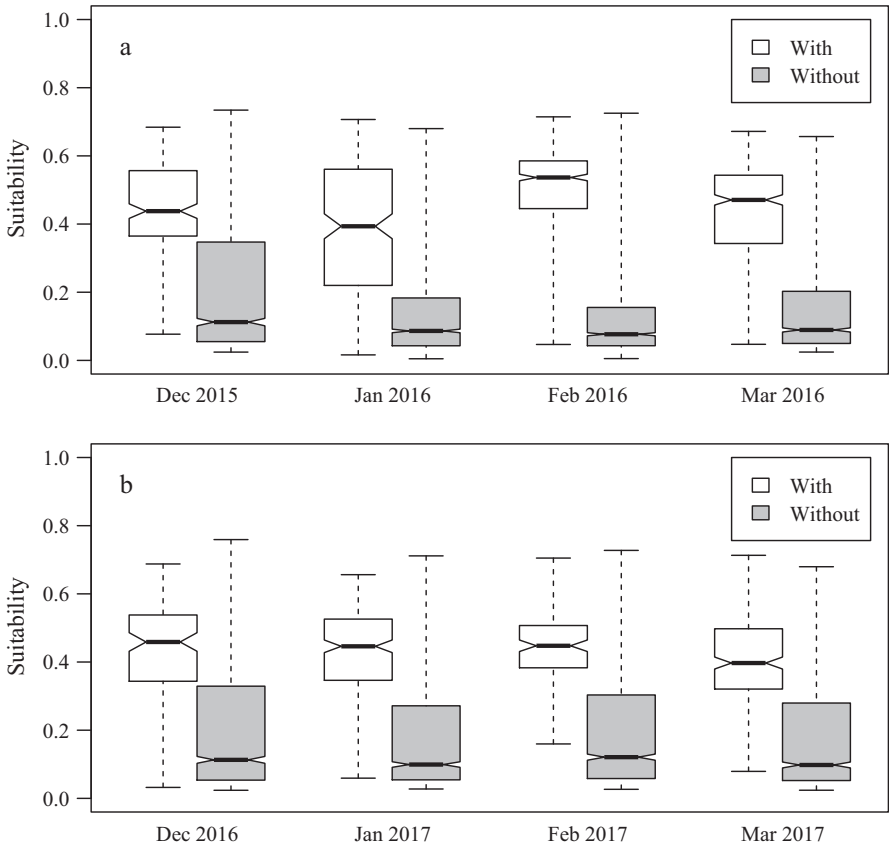

FIG. 4. Boxplots showing the distribution of monthly suitability values for fire occurrence projected for the (a) 2015–2016 and (b) 2016–2017 fire seasons (from December until March) in grid cells where three or more hot pixels where subsequently detected (with) and in grid cells with two or fewer hot pixels (without) in the state of Roraima. The lower and the upper limits of the box represent the first and third quartiles, respectively, the horizontal line within the box represents the median, and the vertical bars represent the data range.

using the 0.3 threshold. The false positive rates varied between 0.15 and 0.28 using the 0.3 threshold (Fig. 5).

The ENSO effect on fire occurrence and the distance to roads were the two most effective variables for predicting the distribution of the occurrence data that was set aside for testing, when predictive performance is measured using AUC (Fig. 6). Precipitation and deforestation were the less useful variables to obtain a good fit to the testing data. The response curves (Fig. 7) also show that varying these two variables, as well as rural settlements (the third lowest in the Fig. 6 ranking), while keeping all other variables at their average sample value, causes relatively low changes in the suitability value. The EEI, secondary vegetation and non-forest cover all show positive association with the suitability value, while an abrupt decrease in fire suitability is seen up to approximately 0.4° (~45 km) of distance to roads.

DISCUSSION

Precipitation and fire anomalies

Negative precipitation anomalies were more extensive in January and February 2016 in Roraima than in the same months of 1998, when the last strong El Niño event occurred. According to Jiménez-Muñoz et al. (2016), the record-breaking warming observed during the 2015–2016 ENSO further increased drought severity through an increase in evapotranspiration. These authors found a larger area under extreme drought in the Amazon during the 2015–2016 ENSO compared to the 1997–1998 event based on a drought index. Although precipitation anomaly was quite extensive in January and March 2016 in Roraima, fire anomalies were observed mostly in the regions of the state where there is either high density of roads, rural settlements, secondary vegetation cover or recent deforestation. This pattern is expected since fire in the Amazon is almost entirely human-ignited (Barbosa and Fearnside 2005) and the correlation between fire occurrence in the Amazon and the variables mentioned above was previously acknowledged in the literature (e.g., Nepstad et al. 2001, Alencar et al. 2004, 2015, Aragão et al. 2008, Silvestrini et al. 2011, Barni et al. 2015*b*).

Nevertheless, some scattered grid cells with fire anomaly ≥1 SD are found in regions covered by dense tropical forest where there are no roads, human occupation is composed of sparse riverine populations, and that do

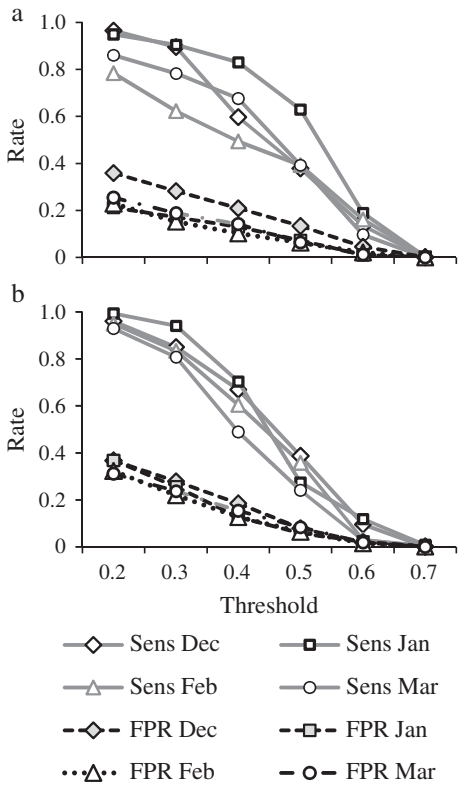

FIG. 5. Sensitivity (Sens) and false positive rate (FPR) for each threshold value considered of the MaxEnt model simulations for the fire seasons of (a) 2015–2106 and (b) 2016–2017 in Roraima State.

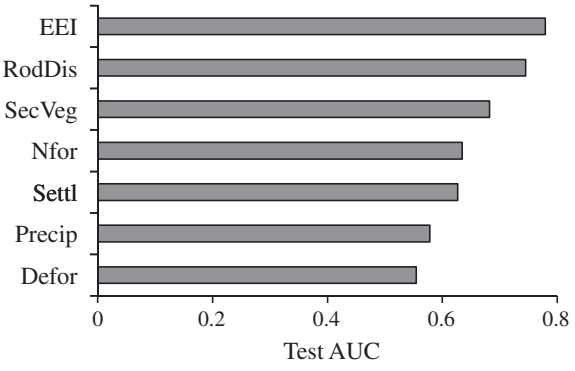

FIG. 6. Results of the jackknife test for evaluating the isolated effect of each variable on the model performance based on the area under the curve (AUC) metric. EEI, ENSO effect index; RodDis, distance to roads; SecVeg, secondary vegetation; NFor, non-forest cover; Settl, rural settlements; Precip, monthly precipitation; Defor, deforestation between August 2013 and July 2014.

not usually burn in Roraima (Barni et al. 2015*b*). Fire occurrence in these regions shows that even a humid dense forest may become flammable and subjected to fires in years of intense drought. We hypothesize that these fires were ignited by traditional subsistence practices that do not represent any forest fire risk in years of normal precipitation.

Precipitation anomaly causes tree-level physiological responses that significantly alter carbon balance in the Amazon, reversing the carbon sink (Aragão et al. 2014, Gatti et al. 2014, Feldpausch et al. 2016). Furthermore, vegetation fires are an important source of carbon to the atmosphere in extreme drought events. Fearnside et al. (2013) estimated that 31.48×10^6 Mg C were emitted from forest fires in the 1997–1998 event in Roraima. According to Aragão et al. (2014), the climatic impacts on forest dynamics and fires together may account for approximately 48.3% of the carbon emissions during extreme drought years in the Brazilian Amazon. Given (1) the current lack of estimates of area burned in different vegetation covers in Roraima during the 2015–2016 drought and (2) the current lack of estimates of the effect of drought on vegetation dynamics and carbon emission/uptake for the savannas, seasonal forests and *Campinaranas* of Roraima, it is difficult to estimate the effect of the 2015–2016 drought on carbon balance in the state. Further studies are necessary to investigate the potentially large effect of the drought and fire anomalies we registered on carbon emissions in Roraima during the 2015–2016 drought.

Modeling fire drivers

Both threshold-dependent and threshold-independent model evaluations indicated satisfactory model performance. Our results concerning model validation during the two analyzed fire seasons are in accordance with the ones found by Fonseca et al. (2016) for the whole Brazilian Amazon in drought and non-drought years, indicating that the model is likely to show good performance in other ENSO and non-ENSO years for Roraima. As pointed out by Fonseca et al. (2016) some commission errors are expected in this modeling approach given that areas suitable for fire occurrence may not burn due to the lack of an ignition source. Additionally, some errors may be related to the fact that we used the precipitation data from the previous month to project fire occurrence. Future studies could test for the accuracy of fire probability prediction with MaxEnt using precipitation-projection data from meteorological models.

Distance to roads and the EEI were the variables that contributed the most to model predictive performance, as measured by the test AUC. The test AUC value of models with only EEI in the present study was similar to the one (0.76) found by Fonseca et al. (2016) for models including only an analogous metric of the effect of the North Atlantic Ocean warming on fire occurrence for the whole Brazilian Amazon. The influence of the sea surface temperature of the Atlantic and Pacific oceans on fire occurrence in the Amazon was previously reported (Chen et al. 2011, Fernandes et al. 2011). It is important to note that the sensitivity of grid cells to changes in MEI, as expressed by the EEI, depends partially on the presence

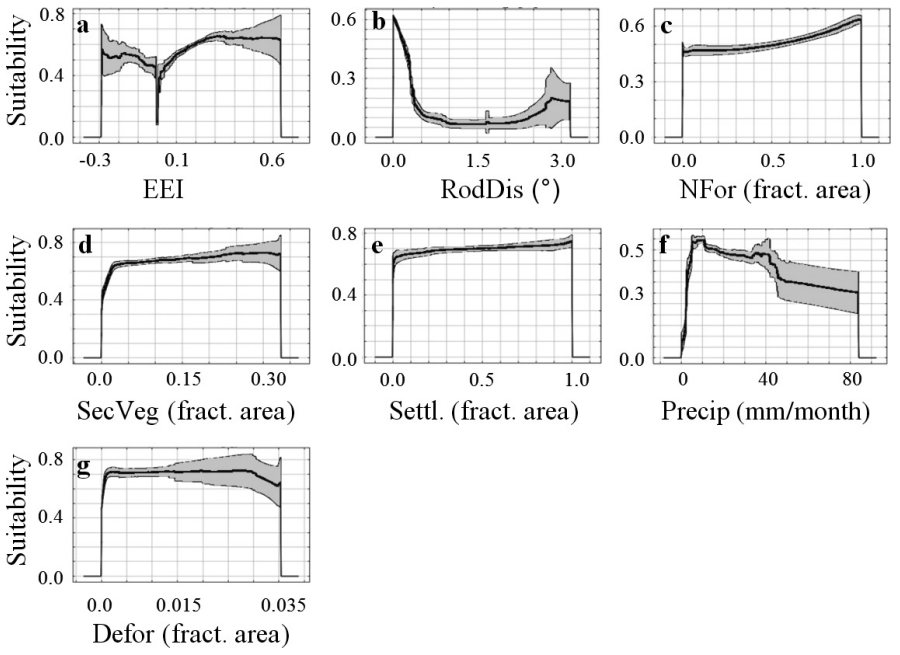

FIG. 7. Response curves showing how each environmental variable affects the suitability for fire occurrence predicted by the MaxEnt model (mean response of 50 MaxEnt runs ± SD). (a) ENSO effect index (EEI); (b) distance to roads (RodDis); (c) non-forest cover (NFor); (d) secondary vegetation (SecVeg); (e) rural settlements (Settl.); (f) monthly precipitation (Precip); (g) deforestation between August 2013 and July 2014 (Defor); fract area is the proportion of each 0.1° grid cell occupied by the land-use or land-cover class.

of ignition sources, given that only grid cells with fire occurrence could present significant correlation with the MEI. This is likely to explain the higher importance of EEI compared to the precipitation itself.

The negative relationship between distance to roads and fire probability is well documented in the literature (e.g., Alencar et al. 2004, Silvestrini et al. 2011) and the drop in fire probability around 45 km is in accordance with the 95th percentile of the distance of MODIS TERRA and AQUA active fire detections to official roads in the Brazilian Amazon documented by Kumar et al. (2014), which varied from 38 km to 51 km between 2003 and 2010.

The positive relationship between fire and both secondary vegetation and non-forest cover in the Amazon, as shown by the response curves, is expected, but less documented at the landscape scale in the literature compared to the other predictive variables mentioned above (Silvestrini et al. 2011, Gutiérrez-Vélez et al. 2014, Fonseca et al. 2016). However, the contribution of secondary vegetation to the model predictive performance was lower than the one (0.81) found by Fonseca et al. (2016). It is important to notice that the secondary vegetation data we used concerns only vegetation regenerating in areas originally covered by forests, and not in areas of native non-forest physiognomies. As the proportion of non-forest vegetation and of seasonal and open ombrophilous forests (which are more fire prone than the dense ombrophilous forest) is higher in Roraima than in the Brazilian Amazon as a whole, it is expected that secondary forest vegetation would show a lower contribution to the model predictive performance when the state is analyzed separately, given that a lower proportion of the training points would be associated with secondary-vegetation areas. Indeed, approximately 25% of the hot pixels detected in January 2016 were in non-forest areas and these areas were not included in the analysis of Fonseca et al. (2016).

It is somewhat surprising that the recent deforestation showed such a low contribution to model performance, contrary to the findings of Fonseca et al. (2016). This can be due to the fact that PRODES monitor the removal of forest vegetation only and no data on clearing of non-forest vegetation is available for Roraima. On the other hand, the distance to the road network is likely to be a proxy of clearing of vegetation, including in the area originally covered by non-forest vegetation, which contributes to its comparative higher importance.

These results highlight the key importance of considering the influence that the planed reconstruction of the BR-319 highway may have on fire occurrence and associated carbon emissions in Roraima. This road connects Porto Velho, the capital of Rondônia state, located in the so-called "arc of deforestation," to Manaus, the capital of Amazonas state, which is already connected to Roraima by the BR-174 road. Its paving, therefore, is likely to foster immigration and deforestation in Roraima, as modeled by Barni et al. (2015*a*). We add to

the Barni et al. (2015*a*) recommendations that, besides the creation of conservation areas, prevention programs should be implemented to avoid the likely increase in forest fires in Roraima in case BR-319 is paved.

The quantification of the precipitation and fire anomalies during the extreme 2015–2016 ENSO provided new information on the dimension of the effect of this event in Roraima and on the effectiveness of current fire control/prevention mechanisms in this important region. Since the 1997–1998 fire event, fire prevention and firefighting actions at all governmental levels (municipal, state, and federal) have improved and have been better integrated, allowing for a scenario of higher institutional governance. This was achieved mainly by the constitution of local multi-institutional committees that undertake daily decisions and firefighting actions during the dry season (Brasil 2016). However, under extreme drought events the spread of fire in Roraima still gets out of control. Our analysis indicates that approximately 38% of the Roraima's area showed positive fire anomaly during the 2015–2016 drought. There is, therefore, still a great need to improve the prevention and combat of forest fires in Roraima. We conclude that MaxEnt and all the publicly available data we used here in model building, including the recently released near-real-time IMERG precipitation data, may help to achieve this objective and therefore minimize fire-related ecosystems degradation, economic losses, and carbon emissions in the state of Roraima.

Acknowledgments

This work was supported by Capes through a postdoctoral fellowship provided to the first author, Amazônica project (http://www.geog.leeds.ac.uk/projects/amazonica; NERC-UK NE/F005806/1), CNPq (grant 458022/2013-6 and Science Without Borders Program) and FAPESP (grant 11/51843-2).

Literature Cited

Alencar, A., L. Solorzano, and D. Nepstad. 2004. Modeling forest understory fires in an eastern Amazonian landscape. Ecological Applications 14:139–149.

Alencar, A., P. M. Brando, G. P. Asner, and F. E. Putz. 2015. Landscape fragmentation, severe drought, and the new Amazon forest fire regime. Ecological Applications 25:1493–1505.

Anderson, L. O., et al. 2015. Disentangling the contribution of multiple land covers to fire-mediated carbon emission in Amazonia during the 2010 drought. Global Biogeochemical Cycles 29:1739–1753.

Aragão, L. E. O. C., Y. Malhi, N. Barbier, A. Lima, Y. Shimabukuro, L. Anderson, and S. Saatchi. 2008. Interactions between rainfall, deforestation and fires during recent years in the Brazilian Amazonia. Philosophical Transactions of the Royal Society B 363:1779–1785.

Aragão, L. E. O. C., B. Poulter, J. B. Barlow, L. O. Anderson, Y. Malhi, S. Saatchi, O. L. Phillips, and E. Gloor. 2014. Environmental change and the carbon balance of Amazonian forests. Biological Reviews 89:913–931.

Arnold, J. D., S. C. Brewer, and P. E. Dennison. 2014. Modeling climate-fire connections within the Great Basin and upper Colorado River basin, Western United States. Fire Ecology 10:64–75.

Bar Massada, A., A. D. Syphard, S. I. Stewart, and V. C. Radeloff. 2013. Wildfire ignition-distribution modeling: a comparative study in the Huron-Manistee National Forest, Michigan, USA. International Journal of Wildland Fire 22:174–183.

Barbosa, R. I. 1993. Ocupação humana em Roraima. II. Uma revisão do equívoco da recente política de desenvolvimento e o crescimento desordenado. Boletim do Museu Paraense Emílio Goeldi 9:177–197. http://agroeco.inpa.gov.br/reinaldo/RIBarbosa_ProdCient_Usu_Visitantes/1993Ocup%20Humana_II_BMPEG.pdf

Barbosa, R. I. 1997. Distribuição das chuvas em Roraima. Pages 325–335 *in* R. I. Barbosa, E. F. G. Ferreira, and E. G. Castellon, editors. Homem, Ambiente e Ecologia no Estado de Roraima. Instituto Nacional de Pesquisas da Amazônia e Governo de Roraima, Manaus, Brazil. http://agroeco.inpa.gov.br/reinaldo/RIBarbosa_ProdCient_Usu_Visitantes/1997DistrChuv%20RR_Livro.pdf

Barbosa, R. I., and P. M. Fearnside. 1999. Incêndios na Amazônia brasileira: estimativa da emissão de gases do efeito estufa pela queima de diferentes ecossistemas de Roraima na passagem do evento "El Niño" (1997/98). Acta Amazônica 29:513–534.

Barbosa, R. I., and P. M. Fearnside. 2005. Above-ground biomass and the fate of carbon after burning in the savannas of Roraima, Brazilian Amazonia. Forest Ecology and Management 216:295–316.

Barbosa, R. I., M. R. Xaud, G. N. F. Silva, and A. C. Cattâneo. 2004. Cinzas na Amazônia: incêndios florestais reencontram Roraima. Ciência Hoje 35:22–27.

Barni, P. E., P. M. Fearnside, and P. M. L. A. Graça. 2015*a*. Simulating deforestation and carbon loss in Amazonia: impacts in Brazil's Roraima State from reconstructing highway BR-319 (Manaus-Porto Velho). Environmental Management 55:259–278.

Barni, P. E., V. B. Pereira, A. O. Manzi, and R. I. Barbosa. 2015*b*. Deforestation and forest fires in Roraima and their relationship with phytoclimatic regions in the northern Brazilian Amazon. Environmental Management 55:1124–1138.

Bolvin, D. T., and G. J. Huffman. 2015. Transition of 3B42/3B43 research product from monthly to climatological calibration/adjustment. https://pmm.nasa.gov/sites/default/files/document_files/3B42_3B43_TMPA_restart.pdf

Brasil. 2016. Operação Roraima Verde 2016. https://queimadas.dgi.inpe.br/ciman/files/relatorios/V952ot26GC42WZQxOPk7KAEkbVRrJW.pdf

Bush, M. B., M. R. Silman, C. McMichel, and S. Saatchi. 2008. Fire, climate change and biodiversity in Amazonia: a Late-Holocene perspective. Philosophical Transactions of the Royal Society B 363:1795–1802.

Chen, F., and X. Li. 2016. Evaluation of IMERG and TRMM 3B43 monthly precipitation products over mainland China. Remote Sensing 8:472. https://doi.org/10.3390/rs8060472

Chen, Y., J. T. Randerson, D. C. Morton, R. S. De Fries, G. J. Collatz, P. S. Kasibhatla, L. Giglio, Y. Jin, and M. E. Marlier. 2011. Forecasting fire season severity in South America using sea surface temperature anomalies. Science 334:787–791.

Couturier, T., A. Besnard, A. Bertolero, V. Bosc, G. Astruc, and M. Cheylan. 2014. Factors determining the abundance and occurrence of Hermann's tortoise *Testudo hermanni* in France and Spain: Fire regime and landscape changes as the main drivers. Biological Conservation 170:177–187.

Davidson, E. A., et al. 2012. The Amazon Basin in transition. Nature 481:321–328.

Diniz, A. M. A., and R. O. Santos. 2005. O vertiginoso crescimento populacional de Roraima e seus impactos socioambientais. Caderno de Geografia 15:23–44. http://www1.pucminas.br/documentos/geografia_25_art02.pdf

Elith, J. 2002. Quantitative methods for modeling species habitat: comparative performance and an application to Australian plants. Pages 39–58 *in* S. Ferson and M. Burgman, editors. Quantitative methods for conservation biology. Springer-Verlag, New York, New York, USA.

Elith, J., S. J. Phillips, T. Hastie, M. Dudik, Y. E. Chee, and C. J. Yates. 2011. A statistical explanation of MaxEnt for ecologists. Diversity and Distributions 17:43–57.

Elvidge, C. D., V. R. Hobson, K. E. Baugh, J. B. Dietz, Y. E. Shimabukuro, T. Krug, and E. M. L. M. Novo. 2001. DMSP-OLS estimation of tropical forest area impacted by surface fires in Roraima, Brazil: 1995 versus 1998. International Journal of Remote Sensing 22:2661–2673.

Fearnside, P. M., R. I. Barbosa, and V. B. Pereira. 2013. Emissões de gases do efeito estufa por desmatamento e incêndios florestais em Roraima: fontes e sumidouros. Revista Agro@ Mbiente On-Line 7:95–111.

Feldpausch, T. R., et al. 2016. Amazon forest response to repeated droughts. Global Biogeochemical Cycles 30:964–982.

Fernandes, K., et al. 2011. North Tropical Atlantic influence on western Amazon fire season variability. Geophysical Research Letters 38:L12701. https://doi.org/10.1029/2011gl047392

Fielding, A. H., and J. F. Bell. 1997. A review of methods for the assessment of prediction errors in conservation presence/absence models. Environmental Conservation 24:38–49.

Fonseca, M. G., L. E. O. C. Aragão, A. Lima, Y. E. Shimabukuro, E. Arai, and L. O. Anderson. 2016. Modelling fire probability in the Brazilian Amazon using the maximum entropy method. International Journal of Wildland Fire 25:955–969.

Gatti, L. V., et al. 2014. Drought sensitivity of Amazonian carbon balance revealed by atmospheric measurements. Nature 506:76–80.

Giovannini, A., D. Seglie, and C. Giacoma. 2014. Identifying priority areas for conservation of spadefoot toad, *Pelobates fuscus insubricus* using a maximum entropy approach. Biodiversity and Conservation 23:427–1439.

Gutiérrez-Vélez, V. H., M. Uriarte, R. DeFries, M. Pinedo-Vásquez, K. Fernandes, P. Ceccato, W. Baethgen, and C. Padoch. 2014. Land cover change interacts with drought severity to change fire regimes in Western Amazonia. Ecological Applications 24:1323–1340.

Huffman, G. J., D. T. Bolvin, and E. J. Nelkin. 2015. Day 1 IMERG final run release notes. NASA Document. http://pmm.nasa.gov/sites/default/files/document_files/IMERG_Final Run_Day1_release_notes.pdf

IBGE. 2012. Manual técnico da vegetação Brasileira. http://biblioteca.ibge.gov.br/visualizacao/livros/liv63011.pdf

INPE. 2016. Monitoramento dos focos ativos nos estados do Brasil. http://biblioteca.ibge.gov.br/visualizacao/livros/liv63011.pdf

Jiménez-Muñoz, J. C., C. Mattar, J. Barichivich, A. Santamaría-Artigas, K. Takahashi, Y. Malhi, J. A. Sobrino, and G. van der Schrier. 2016. Record-breaking warming and extreme drought in the Amazon rainforest during the course of El Niño 2015–2016. Scientific Reports 6:33130.

Kumar, S. S., D. P. Roy, M. A. Cochrane, C. M. Souza Jr., C. P. Barber, and L. Boschetti. 2014. A quantitative study of the proximity of satellite detected active fires to roads and rivers in the Brazilian tropical moist forest biome. International Journal of Wildland Fire 23:532–543.

Lewis, S. L., P. M. Brando, O. L. Phillips, G. M. F. van der Heijden, and D. Nesptad. 2011. The 2010 Amazon drought. Science 331:554.

Liu, Z. 2016. Comparison of integrated multisatellite retrievals for GPM (IMERG) and TRMM multisatellite precipitation analysis (TMPA) monthly precipitation products: initial results. Journal of Hydrometeorology 17:777–790.

Marengo, J. A., C. A. Nobre, J. Tomasella, M. D. Oyama, G. S. Oliveira, R. Oliveira, H. Camargo, L. M. Alves, and F. Brown. 2008. The drought of Amazonia in 2005. Journal of Climate 21:495–516.

Marengo, J. A., J. Tomasella, L. M. Alves, W. R. Soares, and D. A. Rodriguez. 2011. The drought of 2010 in the context of historical droughts in the Amazon region. Geophysical Research Letters 38:L12703.

Martins, F. S. R. V., H. A. M. Xaud, J. R. dos Santos, and L. Soares. 2012. Effects of fire on above-ground forest biomass in the northern Brazilian Amazon. Journal of Tropical Ecology 28:591–601.

Meneses, M. E. N. S., M. L. da Costa, and H. Behling. 2013. Late Holocene vegetation and fire dynamics from a savanna-forest ecotone in Roraima state, northern Brazilian Amazon. Journal of South American Earth Sciences 42:17–26.

Meneses, M. E. N. S., M. L. Costa, D. Enters, and H. Behling. 2015. Environmental changes during the last millennium based on multi-proxy palaeoecological records in a savanna-forest mosaic from the northernmost Brazilian Amazon region. Anais da Academia Brasileira de Ciências 87:1623–1651.

Moritz, M. A., M. Parsien, E. Batllori, M. A. Krawchuk, J. Van Dorn, D. J. Ganz, and K. Hayhoe. 2012. Climate change and disruptions to global fire activity. Ecosphere 3:49.

Murray, F. W. 1967. On the computation of saturation vapor pressure. Journal of Applied Meteorology 6:203–204.

Nepstad, D. C., G. O. Carvalho, A. C. Barros, A. Alencar, J. P. Capobianco, J. Bishop, P. Moutinho, P. Lefevbre, U. L. Silva Jr., and E. Prins. 2001. Road paving, fire regime feedbacks, and the future of Amazon forests. Forest Ecology and Management 154:395–407.

Parisien, M., and M. A. Moritz. 2009. Environmental controls on the distribution of wildfire at multiple spatial scales. Ecological Monographs 79:127–154.

Parisien, M., S. Snetsinger, J. A. Greenberg, C. R. Nelson, T. Schoennagel, S. Z. Dobrowski, and M. A. Moritz. 2012. Spatial variability in wildfire probability across the western United States. International Journal of Wildland Fire 12: 313–327.

Paritsis, J., A. Holz, T. T. Veblen, and T. Kitzberger. 2013. Habitat distribution modeling reveals vegetation flammability and land use as drivers of wildfire in SW Patagonia. Ecosphere 4:53.

Peters, M. P., L. R. Iverson, S. N. Matthews, and A. M. Prasad. 2013. Wildfire hazard mapping: exploring site conditions in eastern US wildland-urban interfaces. International Journal of Wildland Fire 22:567–578.

Phillips, S. J., and M. Dudik. 2008. Modeling of species distributions with Maxent: new extensions and a comprehensive evaluation. Ecography 31:161–175.

Phillips, S. J., M. A. Dudik, and R. E. Shapire. 2004. Maximum entropy approach to species distribution modeling. Pages 655–662 *in* Proceedings of the Twenty-First International Conference on Machine Learning, Banff, Alberta, Canada. Association for Computing Machinery, New York, New York, USA.

Phillips, S. J., R. P. Anderson, and R. E. Shapire. 2006. Maximum entropy modeling of species geographic distributions. Ecological Modelling 190:231–259.

Prakash, S., A. K. Mitra, D. S. Pai, and A. AghaKouchak. 2016. From TRMM to GPM: How well can heavy rainfall be detected from space? Advances in Water Resources 88:1–7.

Ray, D., D. Nepstad, and P. Moutinho. 2005. Micrometeorological and canopy controls of fire susceptibility in a forested Amazon landscape. Ecological Applications 15:1164–1678.

Renard, Q., R. Péllisier, and B. R. Ramesh. 2012. Environmental susceptibility model for predicting forest fire occurrence in

the Western Ghats of India. International Journal of Wildland Fire 21:368–379.

Schroeder, W., I. Csiszar, and J. Morisette. 2008. Quantifying the impact of cloud obscuration on remote sensing of active fires in the Brazilian Amazon. Remote Sensing of Environment 112:456–470.

Schroeder, W., A. Alencar, E. Arima, and A. Setzer. 2013. The spatial distribution and interannual variability of fire in Amazonia. Pages 43–60 *in* M. Keller, M. Bustamante, J. Gash, and P. Silva Dias, editors. Amazonia and global change. American Geophysical Union, Washington, D.C., USA.

Schwartzman, S., et al. 2013. The natural and social history of the indigenous lands and protected areas corridor of the Xingu River basin. Philosophical Transactions of the Royal Society B 368:20120164.

Sharifi, E., R. Steinacker, and B. Saghafian. 2016. Assessment of GPM-IMERG and other precipitation products against gauge data under different topographic and climatic conditions in Iran: preliminary results. Remote Sensing 8:135.

Silvestrini, R. A., B. S. Soares-Filho, D. Nesptad, M. Coe, H. Rodrigues, and R. Assunção. 2011. Simulating fire regimes in the Amazon in response to climate change and deforestation. Ecological Applications 21:1573–1590.

Verbyla, D. L., and J. A. Litvaitis. 1989. Resampling methods for evaluating classification accuracy of wildlife habitat models. Environmental Management 13:783–787.

Xaud, H. A. M., F. S. R. V. Martins, and J. R. dos Santos. 2013. Tropical forest degradation by mega-fires in the northern Brazilian Amazon. Forest Ecology and Management 294:97–106.

Zomer, R. J., A. Trabucco, D. A. Bossio, and L. V. Verchot. 2008. Climate change mitigation: A spatial analysis of global land suitability for clean development mechanism afforestation and reforestation. Agriculture Ecosystems and Environment 126:67–80.

Data Availability

Data available from Figshare: https://doi.org/10.6084/m9.figshare.5393164